Green Chemistry

Role of peracetic acid on the disruption of lignin packing structure and its consequence on lignin depolymerisation

Journal:	*Green Chemistry*
Manuscript ID	GC-ART-06-2021-002300.R1
Article Type:	Paper
Date Submitted by the Author:	21-Aug-2021
Complete List of Authors:	Ma, Ruoshui; Pacific Northwest National Laboratory, Sanyal, Udishnu; Pacific Northwest National Laboratory, PCSD Olarte, Mariefel; Pacific Northwest National Laboratory, Energy and Environment Directorate Job, Heather; Pacific Northwest National Laboratory, Swita, Marie; Pacific Northwest National Laboratory, Jones, Susanne; Pacific Northwest National Laboratory, Meyer, Pimphan; Pacific Northwest National Laboratory Burton, Sarah; Pacific Northwest National laboratory, Environmental Molecular Sciences Laboratory Cort, John; Pacific Northwest National Laboratory, Biological Sciences Division Bowden, Mark; Pacific Northwest National laboratory, Energy Processes & Materials Division Chen, Xiaowen; National Renewable Energy Lab, national bioenergy center Wolcott, Michael; Washington State University Zhang, Xiao; Washington State University , Chemical Engineering and Bioengineering

ARTICLE

Role of peracetic acid on the disruption of lignin packing structure and its consequence on lignin depolymerisation

Received 00th January 20xx,
Accepted 00th January 20xx

DOI: 10.1039/x0xx00000x

Ruoshui Ma,[a †] Udishnu Sanyal,[b,d †] Mariefel V. Olarte,*[a] Heather M. Job,[a] Marie S. Swita,[a] Susanne B. Jones,[a] Pimphan A. Meyer[a], Sarah D. Burton,[c] John R. Cort,[c] Mark E. Bowden,[c] Xiaowen Chen,[e] Michael P. Wolcott,[f] and Xiao Zhang*[a d]

Peracetic acid (PAA) is an effective oxidant capable of solubilising lignin and efficiently depolymerising it to selective phenolic compounds; however, the specific role by which PAA initiates the depolymerisation is still elusive. Herein, interaction between PAA and the lignin macromolecule and the consequent structural changes of the latter were studied by characterising the lignin packing structure and its associated changes during the oxidation process. While the lignin packing structure and its changes associated with the PAA-mediated oxidation was probed by X-ray diffraction, impact of the PAA on different chemical functionalities present in the lignin structure was established by ^{13}C and ^{1}H-^{13}C heteronuclear single-quantum coherence nuclear magnetic resonance (NMR) spectroscopy. Combining the NMR spectroscopy results, and the product distribution, we conclude that the predominant reaction pathway for the oxidative depolymerisation of lignin with PAA is the Baeyer-Villiger oxidation of the ketone formed by the oxidation of the benzylic hydroxyl group adjacent to the β-O-4 linkage. The experimental evidence provided herein corroborated that PAA instigates oxygen insertion to the lignin macromolecule resulting in disruption of its packing structures and facilitates depolymerisation. We also investigated various metal oxide and mixed metal oxide catalysts to identify effective catalysts that further enhance the efficiency of PAA mediated depolymerisation of lignin and produce selective monomeric phenolic compounds. Techno-economic analysis was also conducted to identify the key parameters associated with this oxidative process that need to be considered for possible commercial application.

Introduction

Lignin, a natural aromatic biopolymer (15-30% by weight, 40% by energy), is the largest source of renewable aromatics on earth and thus represents an attractive feedstock for renewable fuel, chemicals, and materials synthesis. However, due to its structural heterogeneity and complexity, development of a selective and efficient lignin depolymerisation technology remains a challenge.[1-10] Among the various lignin depolymerisation technologies, oxidative lignin depolymerisation has shown distinctive advantages such as relative mild reaction conditions (low temperature and pressure), high conversion, and selectivity.[5, 11-18] The lignin oxidation chemistries have been widely applied in modern wood pulping and bleaching processes.[12]

Most concurrent research efforts focused on the development of efficient lignin depolymerisation chemistries by cleaving the ether linkages, considered to be the predominant type of linkage, in native lignin. However, considering only ether cleavage, most lignin depolymerisation processes are limited in terms of monomer yield that are in the range of 5-20 mol%.[2, 8, 19] Only few reports are available with monomeric phenolic yield ~50 mol%;[16, 19-21] thus an efficient strategy capable of both ether (C-O) and carbon-carbon (C-C) cleavages is essential to achieve high yield of monomeric phenolic compounds (MPCs). Oxidative depolymerisation of lignin has shown a promising potential to be capable of cleavage of C-O linkages, C-C linkages, and even the aromatic rings leading to high recoveries of various monomeric products.[5, 16, 22-30]

Among many oxidants, peracetic acid (PAA) is recognised as environmentally benign with a high oxidation potential (1.748 V vs. Standard Hydrogen Electrode).[14, 21, 31-39] PAA was recently touted as the greener alternative to sodium hypochlorite and chlorine dioxide for disinfecting wastewater streams.[40, 41] As decomposition of PAA produces only acetic acid, oxygen, and water, there is little need for removal or neutralisation before the clean water enters the waterways, thus showing environmental and economic promise. An earlier paper[35] showed the usage of PAA to depolymerise biorefinery lignin and

[a.] Energy and Environment Directorate, Pacific Northwest National Laboratory, 902 Battelle Boulevard, Richland, WA 99354, USA.
[b.] Physical and Computational Sciences Directorate, Pacific Northwest National Laboratory, 902 Battelle Boulevard, Richland, WA 99354, USA.
[c.] Earth and Biological Sciences Directorate, Pacific Northwest National Laboratory, 902 Battelle Boulevard, Richland, WA 99354, USA.
[d.] Voiland School of Chemical Engineering & Bioengineering, Washington State University, Richland, WA, 99354, USA.
[e.] National Bioenergy Centre, National Renewable Energy Lab, Golden, CO, 80127 USA.
[f.] Composite Materials Engineering Centre, Washington State University, P. O. Box 645815, Pullman WA 99164 USA.
† First two authors contributed equally.
Electronic Supplementary Information (ESI) available: [details of any supplementary information available should be included here]. See DOI: 10.1039/x0xx00000x

produce selective MPCs. By controlling the reaction conditions, it was also demonstrated that PAA can oxidise the aromatic rings to produce dicarboxylic acids, an important building block to produce several biopolymers, further diversifying the product portfolio of this oxidation process. Thus, its ability to cleave both C-C bond and ether-linked phenylpropane units makes PAA oxidation distinctive from most other lignin depolymerisation chemistries.[16, 21, 42]

Despite its high activity for catalysing lignin depolymerisation, the precise mechanism of how PAA interacts with lignin macromolecules and consequently, how PAA effects the cleavages of lignin bonds is still lacking. This study applies nuclear magnetic resonance (NMR) spectroscopy and X-ray diffraction (XRD) to gain an understanding of the underlying mechanism corresponding to PAA-mediated disruption of the lignin packing structure and its subsequent depolymerisation. It was also found that usage of metal oxide catalyst (i.e. niobium pentoxide) in conjunction to PAA further increases delignification efficiency and selectivity.[35] We then selected and investigated 15 metal oxide and mixed-metal oxide catalysts in addition to niobium pentoxide for lignin depolymerisation. Lastly, we also reported the results of a preliminary techno-economic analysis that identified key cost drivers that needed to be considered towards a cost-effective technology.

Experimental section

Lignin purity determination

Diluted acid corn stover lignin (DACSL) was collected from the deacetylation and disc refining pre-treatment of corn stover to produce carbohydrates (provided by the National Renewable Energy Laboratory, Colorado, USA)[43]. Following alkali purification, DACSL was utilised as the feedstock for the present study as prior reports showed that it possessed high reactivity for PAA-mediated depolymerisation.[21, 35, 44] The lignin purity and residual carbohydrate content were determined by Klason lignin analysis (Table S1).[45] Lignin purity was calculated based on the total amount of acid-soluble lignin and acid-insoluble lignin in samples, as determined according to published procedures.[46]

General oxidation procedure

Oxidation of DACSL (~50 mg) by PAA were conducted at different temperatures (room temperature or 60°C), reaction times (0-18 h), and PAA dosages (0-1 g PAA per g lignin). Different conditions were chosen to address different research questions as stated in the main text. During the reported catalyst screening, lignin, PAA (diluted with acetic acid), and catalysts were mixed (THERMO SCI TYPE 16700 MIXER, Fremont, CA) at the selected reaction temperature A ratio of 1:10 by weight catalyst to DACSL (50 mg) and 1:5 by weight PAA to DACSL were added into the mixture prior to the reaction. The microtubes were then heated and allowed to react at 60 °C for 5 h. The impact of PAA on the disruption of lignin packing structure was done at room temperature for different time intervals, such as 1, 3, 5 and 18 h. The reaction mixture was quenched by addition of ~30 g deionized (DI) water. A solid residue was isolated after centrifugation and washed with DI water (~ 20 g each time) for 3 times. Dark to light brown color (corresponding to low to high degree of oxidation respectively) solid was finally obtained after freeze drying.

Analysis of oxidation products

The yield of the total amount of MPCs in the reaction solution were quantified via microtiter-plated Folin-Ciocalteu (F-C) assay following previously published methods.[35, 44, 47, 48] Samples were taken from the reaction mixtures and reacted with the F-C reagent in a 96-well microtiter plate. To each well was added 150 µL of water, 10 µL of F-C reagent, and 2 µL of the proper dilution of test compound. The contents of the wells were stirred and allowed to stand for 5 min. After this, 30 µL of a 20% aqueous sodium carbonate solution was added to each well. The contents of the wells were again incubated at 45°C for 30 min in a dry bath. The absorbance of the aliquots at 765 nm after the reaction with F-C reagent was measured against a blank using deionised water. The amount of MPCs was quantified by correlating the sample absorbance with the MPC concentration using a standard curve generated from isoeugenol (as standard compound) at different concentrations.

When lignin was treated with 0.1 g PAA/g lignin and 0.2 g PAA/g lignin in acetic acid, the MPCs are present in the solution while non-depolymerised oligomers were obtained as solid residues. The reported yield in the present work corresponds to the amount of MPCs present in the solution. The mass balance obtained as 90.8% and 80.2% corresponding to the oxidation reaction by using 0.1 g PAA/g lignin and 0.2 g PAA/g lignin, respectively, suggests that the use of F-C method is satisfactory in determining the yield of phenolic compounds. The detailed calculation corresponding to mass balance of these systems are provided in the supporting information and Table S2. The lower mass balance obtained with 0.2 g PAA/g lignin could be due to a relatively higher oxidation rate leading to the formation of a higher fraction of non-lignin derived soluble compounds.

To further analyse the product selectivity, ethyl acetate (Sigma Aldrich, high performance liquid chromatography or HPLC grade, 99.8%) was used to extract the phenolic compounds from the reaction solution. Typical extraction procedure includes the addition of 2 mL ethyl acetate to 1 mL of aqueous sample, after which, the mixture was shaken vigorously for 5 min using an external shaker. Upon separation from the aqueous layer, the ethyl acetate fraction was collected and stored in a separate vial. The extraction procedure was repeated thrice and finally the ethyl acetate fractions (~6 mL) were combined and dried under a stream of air using a Pierce ReactiVap apparatus (Thermo Scientific, Fremont, CA) to remove the solvent prior to the trimethylsilylation (100 µL of 10% trimethylchlorosilane with *N*,*O*-bis(trimethylsilyl) trifluoroacetamide). The silylated ethyl acetate fraction was analysed by a gas chromatograph mass spectrometer (Agilent 7890 A/5975C) equipped with a DB-5 capillary column. The following oven program was utilised: initial temperature at 100°C, held for 3 min at temperature, followed by a

5°C min^{-1} ramp to 200°C, held for 3 min at temperature, and then followed by a 20°C min^{-1} ramp to 320°C, held for 10 min at temperature. The mass spectrometer detector was run on positive EI mode with temperature settings as follows: MS Source Setpoint at 230°C and MS Quad Setpoint at 150°C. Solvent delay was set to 3 min and the compounds between 5 and 30 min were identified and quantified. Scanning ion range was set from *m/z* 50–1000. The product selectivity was determined based on total ion chromatogram (or TIC) peak areas.

X-Ray diffraction

Structural characterisation of lignin and partially oxidised lignin samples by XRD was conducted on a Panalytical MPD diffractometer using Cu Kα radiation (λ = 1.54184 Å) and a variable divergence slit in Bragg-Brentano geometry. Each sample was packed in a zero-background holder and scanned in the range 2θ = 5-100°. Deconvolution of the spectra was conducted with pseudo-Voigt profiles using TOPAS v6 (Bruker AXS).

^{13}C NMR, ^{1}H-^{13}C HSQC NMR

Lignin and partially oxidised lignin samples were acetylated according to a previously reported method[49] and dissolved in DMSO-d_6 (100 mg sample per 0.6 ml DMSO-d_6). One-dimensional ^{13}C NMR spectra of lignin samples were obtained at 298 K on a 500 MHz Agilent DD2 spectrometer. The pulse sequence utilised a 9.5 µs 90° pulse followed by 1 s of WALTZ decoupling during the acquisition time. The recycle delay was 10 s and the chemical shift was referenced to the solvent peak at 39.5 ppm. The peaks were assigned according to previous studies.[50, 51]

The two-dimensional heteronuclear single quantum coherence (HSQC) NMR spectra of the acetylated lignin and acetylated partially oxidised lignin were acquired at 298 K on a 500 MHz Varian Inova spectrometer equipped with a room temperature Varian HCN probe. Samples (ca. 50 mg) were dissolved in 600 µL DMSO-d_6. Two-dimensional ^{1}H-^{13}C HSQC (gChsqc.c) spectra were acquired for aliphatic and aromatic regions separately with tCH tuned for 1JCH = 140 Hz (aliphatic C-H) or 172 Hz (aromatic C-H), and with spectral widths of 17 ppm in the directly detected dimension (^{1}H) and 90 ppm or 60 ppm for aliphatic or aromatic regions, respectively, of the indirectly detected dimension (^{13}C) centred correspondingly at either δ_C 51 ppm or 121 ppm. Spectra were acquired with 1024 complex points in the ^{1}H dimension and 768 complex points (States-TPPI mode) in the ^{13}C dimension. Spectra were processed in MestReNova version 14, with cosine bell apodization and 2X zero-filling in both dimensions and referenced to residual ^{1}H in the DMSO solvent (δ_H 2.50 ppm and δ_C 39.5 ppm).

Results and discussion

Disruption of lignin packing structure by PAA mediated oxidation

Packing structure integrity was often considered as one of the significant factors that prevents the effective depolymerisation of lignin. During lignin biosynthesis, the overall transformation of glucose to monolignols and subsequent lignin macromolecules is an electron-gaining or reductive process.[3, 52] The highly electron-dense aromatic skeleton and the oxygen-functionalised side chains impose various non-covalent interaction (e.g. π-π interaction, hydrogen bond) and stabilises the packing structure of lignin. We observed that upon addition of PAA (1 g PAA/g lignin) to DACSL at 60°C, the solid lignin powders first swelled into a fluffy brown-colored form and shortly after that, the DACSL was completely dissolved into the solution (typically less than an hour). This intriguing observation that PAA is capable of dissolving solid lignin indicated that the polymeric structure of lignin undergoes certain physical and chemical changes prior to its depolymerisation. However, as we show in our results section, only a portion of the completely dissolved lignin yielded MPCs.

To understand this phenomenon in more detail, we carried out partial oxidation of lignin using a lower PAA dosage (0.2 g PAA/g lignin, approximately 0.5 mole PAA per mole of lignin equivalent) and at mild condition (room temperature). We quenched the reaction at different time intervals such as 1, 3, 5, and 18 h and labelled as LO-1 (quenched after 1 h), LO-2 (quenched after 3 h), LO-3 (quenched after 5 h), and LO-4 (quenched after 18 h), respectively, as shown in Figure 1.

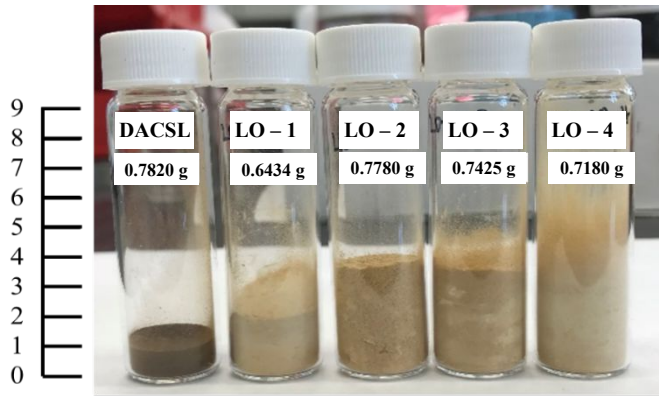

Figure 1. Partially oxidised lignin samples obtained at different time intervals. Samples of similar weight were utilised to compare their respective volume. Reaction condition: 0.2 g PAA/g lignin, room temperature, acetic acid as solvent. DACSL – parent lignin; LO-1 – reaction quenched after 1 h; LO-2 – reaction quenched after 3 h; LO-3 – reaction quenched after 5 h; LO-4 – reaction quenched after 18 h.

Compared to the original DACSL with similar weight, the volume of LO-1 and LO-2 lignin increased two to three times respectively. Further increase in reaction time to 5 and 18 h resulted in only small expansion of the volume. During this treatment, small amounts of soluble products were generated. The ability of PAA to swell lignin's structure indicated that the oxidant significantly modified the physio-chemical interactions present in lignin macromolecules and resulted in exfoliation of the packing structure. It is also important to note that changing the solvent from acetic acid to 1,4-dioxane or n-hexane did not change the swelling effect (Figure S1, Table S3 and Figure S2,

Table S4 respectively). This observation further confirmed the major role of PAA that causes the structural changes of lignin.

Exfoliation of the lignin packing structure and its structural changes imparted by PAA was probed by powder XRD. Earlier studies also utilised powder XRD as a tool to investigate the changes of lignin packing as a result of chemical modification or diffusion into other materials.[53-55] It is apparent that being a relatively amorphous material, powder patterns of lignin are devoid of sharp peaks characteristic of long-range order. However, some short-range order is evident from the broad peaks in the XRD patterns, and the modification of these peaks was utilised to follow the impact of oxidation on lignin packing. Li and Sarkanen[56] have described how the intense peak near 4.0 Å can be assigned to the perpendicular distance between aromatic rings that are approximately parallel to one another. In the present study, we focus on the changes in interplanar distance because we hypothesized it to vary due to the change in lignin close pack structure during PAA mediated oxidation.

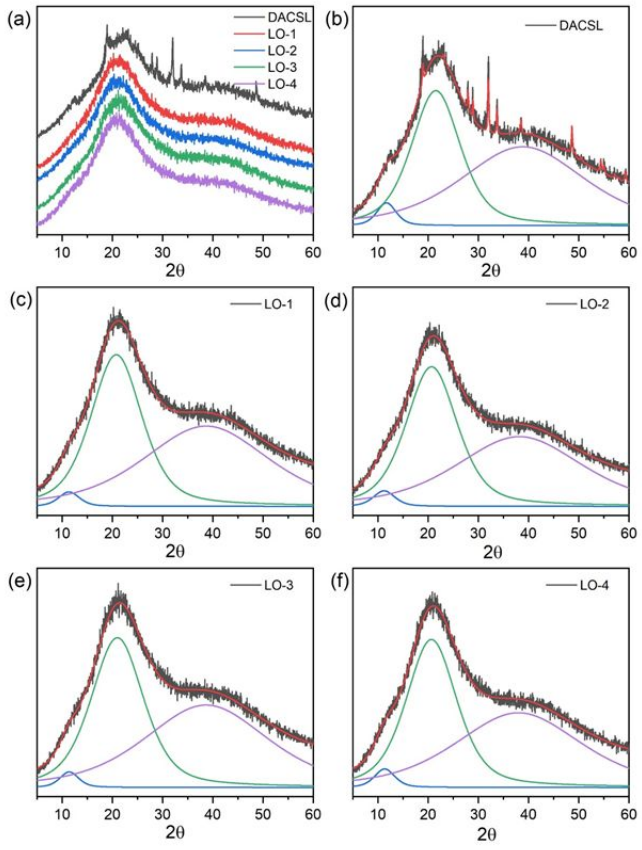

Figure 2. (a) Comparison of powder XRD of different partially oxidised lignin samples along with the parent DACSL. Powder XRD pattern and corresponding multi-peak deconvolution of (b) DACSL; (c) LO-1; (d) LO-2; (c) LO-3; (d) LO-4.

Figure 2a compares the XRD patterns of partially oxidised lignin samples to the parent DACSL. Deconvolution of the broad peaks is shown in Figure 2b-f, with the sum of the peaks (red line) laid over the experimental pattern (black line) to demonstrate the quality of the fit. XRD peak fitting and the corresponding analysis was carried out to examine the changes during oxidation and compare them across different oxidative treatments.

The parent DACSL contains small crystalline peaks arising from Na_2SO_4, which was also fitted in this sample (Figure S3). These crystalline peaks are likely formed during freeze-drying and came from residual salts from the NaOH and H_2SO_4 reagents that were previously utilised in the deacetylation and mild hydrolysis to remove the carbohydrates in the DACSL. The large broad feature in the XRD patterns near 2θ = ~21° shifted slightly toward smaller diffraction angles (larger d-spacing) because of the PAA treatment. The observed d-spacings were 4.12, 4.27, 4.29, 4.23, and 4.30 Å, respectively, for samples in the order from DACSL to LO-4. This shift was attributed to a weakening of the non-covalent forces between the approximately parallel aromatic rings of neighbouring lignin molecules.[56] The peak breadth also increased from a full width at half-maximum of 10.6° 2θ in the parent DACSL to 11.0 – 11.4° in the treated samples, indicating a larger range of stacking environments. The changes observed by XRD were consistent with the volume expansion of solid lignin observed after PAA treatment (Figure 1).

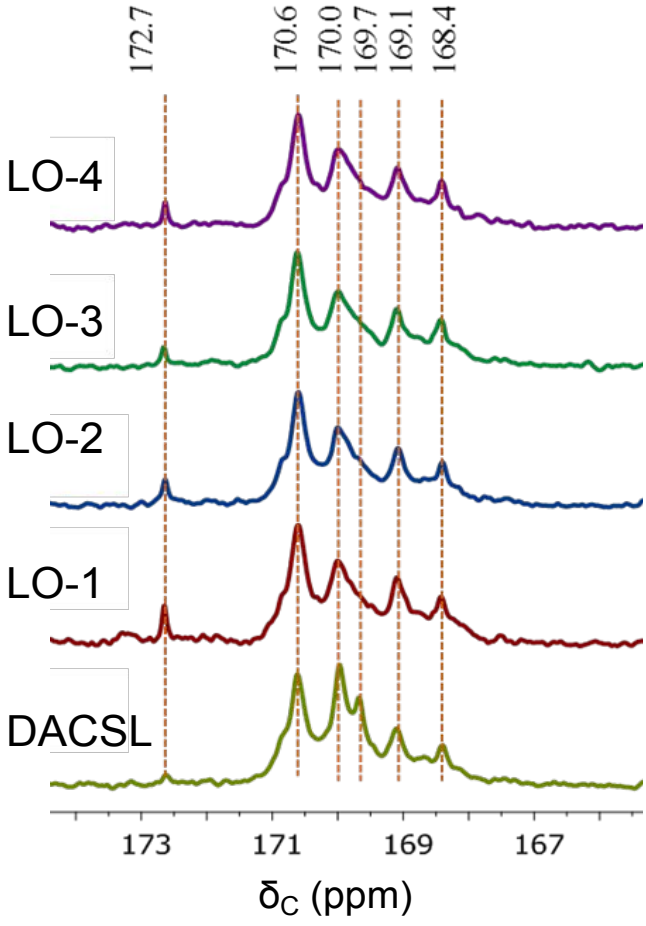

Figure 3. ^{13}C NMR spectra of acetylated DACSL and PAA-oxidised lignin samples obtained at different time intervals.

The chemical changes imparted on the lignin structure because of PAA-mediated oxidative treatment were established by NMR spectroscopy. Both the parent DACSL and the

corresponding oxidised samples (LO-1 to LO-4) were characterised using ^{13}C NMR and 2-D ^{1}H-^{13}C HSQC NMR. Assignments of the different signals obtained herein were made according to previous literature.[57] Figure 3 shows the ^{13}C NMR spectra of acetylated DACSL and different oxidised samples (LO-1 to LO-4). The region at 175-165 ppm was chosen for the analysis as it consists of the carbonyl carbon attached after acetylation of the primary and secondary hydroxyl groups which are expected to be more sensitive towards oxidation. The region also includes the information regarding certain carbonyl group in acid and ester moieties. The ^{13}C NMR spectra of DACSL and the various oxidized samples are shown in Figure S4-S8.

The chemical shift (δ_C) corresponding to the aromatic carbons was obtained between 102 and 160 ppm and integration of these peaks were set as 6.0 because of the six carbons on each aromatic ring. Accordingly, the integration of the peaks at δ_C 171.2–170.2 ppm, 170.2–169.5 ppm, and 169.5–168.0 ppm represented the number of carbonyl carbons attached to acetylated primary, secondary and phenolic hydroxyl groups respectively per aromatic rings in different lignin samples (Table S5). The full spectra of the ^{13}C NMR were presented in Figures S5-S9. The peak at δ_C 170.6 ppm was assigned to the carbonyl carbon of the acetyl group attached to the primary -OH group. The number of primary hydroxyl groups per aromatic ring was obtained as ~0.6 after the PAA treatment. On the other hand, peaks at 169.7 and 170.0 ppm, assigned to the carbonyl carbon in acetylated secondary -OH group on lignin propanyl side chains, were notably flattened after PAA treatment. Integration of these two peaks showed that ratio of secondary hydroxyl groups per aromatic ring reduced from 0.63 in DACSL to 0.58 (LO-1), 0.55 (LO-2), 0.55 (LO-3), and 0.55 (LO-4), respectively. The decrease in peaks corresponding to the secondary hydroxyl groups compared to the primary suggests that the former was more reactive towards oxidation in the current reaction condition. According to the NMR data, we concluded that maximum changes in the lignin structure due to the PAA was noted after 3 h of oxidation. The conclusion fits well with the swelling phenomena of lignin (as shown earlier) which also shows that maximum volume expansion was obtained after 3 h. The peaks at 169.1 ppm and 168.4 ppm, which were assigned to carbonyl carbon in acetylated phenolic

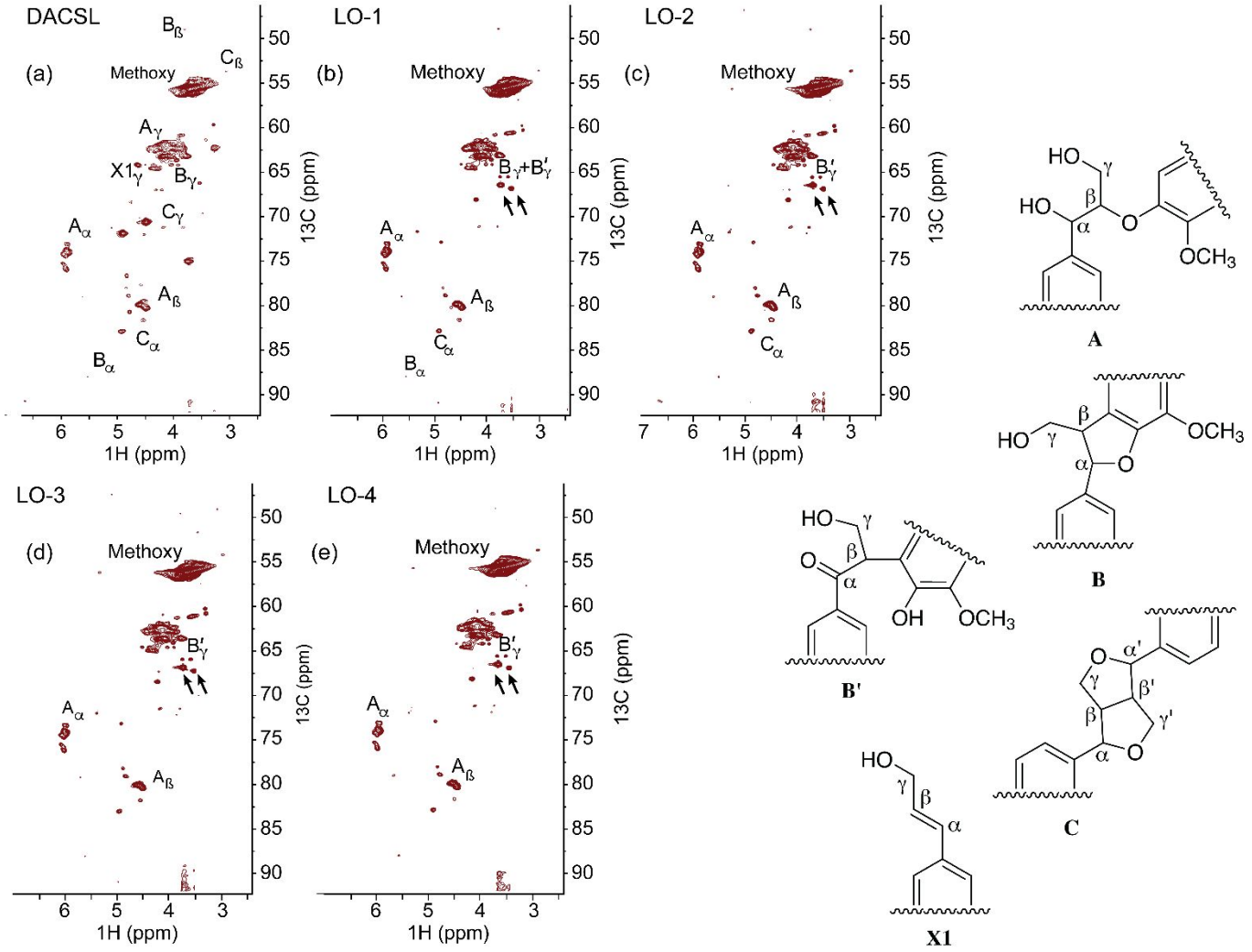

Figure 4. ^{1}H-^{13}C HSQC NMR spectra of partial oxidised lignin compared to DACSL. The blue arrow shows the emergence of the new peaks because of the oxidative treatment. The main structural units assigned were shown with their structures on the right.

ARTICLE

hydroxyl groups were increased along the treatment. The ratio of phenolic hydroxyl group to aromatic ring calculated from the integration of the corresponding peaks in DACSL was 0.42. This value was increased to 0.55 in LO-1 (1 h oxidative treatment) suggesting the cleavage of β-O-4 ether linkages and the consequent production of free phenolic hydroxyl groups. However, the ratio of phenolic hydroxyl group/aromatic ring did not change significantly with longer PAA treatment. The corresponding values obtained were 0.52, 0.54, and 0.56 for LO-2, LO-3, LO-4 respectively, suggesting that β-O-4 ether linkages were stabilised after extended exposure to PAA.

The chemical changes in the lignin structure, specifically to the inter-unit linkages, was further investigated by using ^{1}H-^{13}C HSQC NMR. All the assignments were based on dimeric model compounds as reported in previous literature.[57] We specifically investigated the aliphatic oxygenated side-chain regions (δ_C/δ_H=90-45/6.5-2.5 ppm/ppm) in detail (Figure 4).

Figure 4a shows the HSQC NMR spectra of DACSL prior to PAA treatment. The different functionalities such as β-aryl ether (β-O-4, **A**), phenylcoumaran (β-5, **B**), resinol (β-β, **C**) linkages, and cinnamyl alcohol structures (**X1**) were identified in DACSL. The peaks corresponding to these interlinkages diminished gradually at different rates. Cinnamyl alcohol structure (**X1**) was the most labile and reacted completely within 1 h (Figure 4b). The signal corresponding to phenylcoumaran (β-5, **B** in Figure 4) and resinol (β-β, **C** in Figure 4) linkages were gradually reduced, accompanied by the emergence of new peaks as identified in Figures 4b-4e, suggesting the deconstruction of the five-member ring containing the ether linkages. The significant reduction of the peak corresponding to the β-aryl ether (β-O-4, **A**) along with the emergence of new peaks (shown by blue arrows in Figure 4) further confirmed the conversion of β-O-4 linkages. According to this NMR data , we hypothesized that the oxidative conversion of the hydroxyl groups on C_α (δ_C/δ_H=73.8/5.9 ppm/ppm in **A**, δ_C/δ_H=87.8/5.5 ppm/ppm in **B**, δ_C/δ_H=82.7/4.9 ppm/ppm in **C**) and the changes associated with hydroxyl groups on C_γ (δ_C/δ_H=62/4.1 ppm/ppm in **A**, δ_C/δ_H=63.5/4.0 ppm/ppm in **B**, δ_C/δ_H=70.9/4.2-3.8 ppm/ppm in **C**) significantly reduces the possibility of forming intra- and inter-molecular hydrogen bonds. Additionally, PAA mediated oxidation generally leads to the formation of large functional groups i.e., carboxylic acids (see the discussion corresponding to the reaction mechanism) which could impose steric constraint and prevents the π-π interaction between lignin aromatic rings, thus contributing to the observed swelling effects.

Combining the physical changes in the lignin structure along with the spectroscopic evidence (XRD, ^{13}C NMR, and HSQC NMR), we confirmed that PAA oxidatively modified the lignin packing structure which was exhibited by the volume expansion of solid lignin. We propose that exfoliation of the lignin packing structure is the primary step that makes lignin more accessible for further depolymerisation. The oxidative modification of lignin propanyl side chain activates both the C-O bond in ether linkage and C-C bonds, and consequently facilitates depolymerisation. Recently, Rahimi et al. also postulated that oxidative modifications of the aliphatic hydroxyl group to carbonyl promoted the cleavage of β-O-4 ether linkage.[20, 58] Effective cleavage of β-aryl ether linkages by PAA to produce phenolic compounds was also demonstrated by using model compound, 1-(4-hydroxy-3-methoxyphenyl)-2-(2-methoxyphenoxy) propanol.[35, 39]

Effect of PAA dosages for depolymerisation of DACSL

We next turn our focus to investigate the effect of PAA dosage on the efficacy of lignin depolymerisation and determine the various phenolic compounds obtained in the product stream. F-C analysis[35, 44, 47, 48] was carried to determine the total yield of phenolic compounds based on conversion of Klason lignin using isoeugenol as a calibration standard.[48, 59] The product selectivity was investigated using gas chromatography mass spectroscopy. An experiment without PAA was carried out as baseline. Figure 5 presents the effect of PAA dosage (0-1.0 g PAA/g lignin) on total yield of phenolic compounds and product selectivity during the depolymerisation of DACSL at 60°C. It is important to mention here that all these reactions were carried out for 5 h as major structural changes of lignin were accomplished within 3 h.

Increasing PAA amount from 0 to 0.8 g PAA/g lignin resulted in a continuous increase in the yield of phenolic compounds from 9 wt% to 32 wt% (Figure 5, yellow line). However, further increasing the PAA amount to 1 g/g lignin resulted in the small reduction of phenolic compounds yield, suggesting an optimised amount of PAA (0.8 g/g lignin) is required to depolymerise lignin. Minor amounts of phenolic compounds produced in case of 0 g PAA/g lignin was attributed to the hydrolysis of ester linkages of the coumaric acid derivatives (e.g., p-coumaric acid, ferulic acid). It is shown in the precedent literature that corn-stover lignin (used in the present study) contains ~10-20% of coumaric acid fraction and thus corroborates well with the amount of hydrolysis product.[21]

Detailed analysis of reaction products showed that the product selectivity also changed notably along with the increase

in PAA dosage from 0 g PAA to 1 g PAA/g lignin (Figure 5, stacked columns). Without the addition of PAA (i.e. 0 g PAA), p-coumaric acid derivatives (p-coumaric acid and ferulic acids) were identified as the predominant phenolic products, representing 87% of the total products (Figure 5, stacked columns, green). Monomeric hydroxylated phenolics (11%, Figure 5, dark green) and monomeric phenolic acids (77%, Figure 5 green) were obtained as major products when the amount of PAA was increased to 0.5 g/g lignin. Among the various phenolic acids obtained herein, ~60% was comprised of coumaric acid derivatives wherein the rest were identified as vanillic and syringic acid. C2-C4 side-chain fragments (e.g. oxalic acids, propanedioic acids, 2,3-dihydroxylpropanoic acid, shown in blue in Figure 5) were also detected and likely resulted from side chain cleavage (detailed mechanism will be discussed below). Selectivity of 88% was achieved by combining the yield of monomeric hydroxylated phenolics and phenolic acids. Small

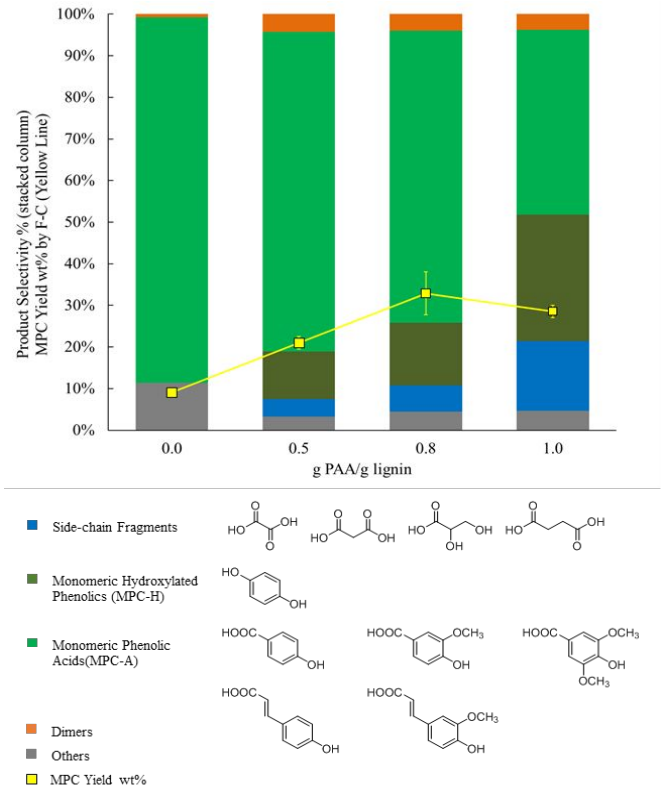

Figure 5. Effect of PAA dosage (0-1.0 g PAA/ g Lignin) on total yield of phenolic compounds different product selectivity obtained during PAA-mediated depolymerisation of lignin at 60°C for 5 h.

amounts of dimers (4%, Figure 5, orange) were also detected in this case.

Further increasing PAA dosage to 0.8 g PAA/g lignin led to an increase in monomeric hydroxylated phenolics (15%) while selectivity to monomeric phenolic acids dropped to 70%. However, the overall selectivity to MPCs was very similar (85%) to that obtained in the case of 0.5 g PAA/g lignin. Both side-chain fragments (~6%) and dimers (~4%) were also identified in the product stream. Increasing the oxidant (PAA) dosage to 1.0 g PAA/g did not increase the MPC yield but affected the product selectivity. Significant amounts of monomeric hydroxylated phenolics (selectivity ~30%) were obtained in this case. The selectivity to the products formed due to the fragmentation of the sidechain was notably increased (~18% selectivity). Decrease in both MPC yield and selectivity with increase in PAA dosage from 0.8 g PAA/g lignin to 1.0 g PAA/g lignin could be attributed to the presence of excess PAA, which led to the over-oxidation of phenolic compounds to benzoquinone /polymerised quinone, or ring-cleavage products.

Reaction mechanism pertaining to the PAA-mediated depolymerisation of lignin to MPCs

Based on the products obtained during the PAA-mediated oxidation of lignin, the underlying reaction mechanism pertaining to the cleavage of C-C linkages is classified in two major pathways,[12, 14, 35, 39, 60, 61] that is (i) side-chain replacement (top panel, Scheme 1) and (ii) side-chain oxidation (bottom panel, Scheme 1). We propose that the side chain replacement pathway proceeds through aromatic electrophilic substitution of hydroxonium ion, OH^+, produced *in situ* due to the heterolytic cleavage of the peroxide bond of PAA. Initial attack of the OH^+ ion to the phenyl ring and subsequent displacement of the alkyl side chain resulted in ring hydroxylation, thus, producing a substituted phenolic compound (**1**). The detailed stepwise reaction mechanism is shown in Scheme S1. The presence of hydroxonium ion as an active species during the PAA-mediated oxidation of aromatic compounds was also invoked earlier.[12, 35] On the other hand, side-chain oxidation proceeds through oxidation of the benzylic hydroxyl (or secondary hydroxyl group as described in an earlier section) group present in C_α to produce the ketone (**2**). Oxidative modification of lignin side chain accompanied by the transformation of benzylic hydroxyl group to the corresponding ketone in the presence of different catalysts was also reported in earlier studies.[20, 58, 62-64] Under oxidative condition, the phenyl propane unit could also undergo C-O (C_β-O) cleavage to form pinacol derivative that subsequently undergoes pinacol-pinacolone rearrangement to produce an unsymmetrical ketone (**4**). While C-O cleavage (β-O-4) was established by ^1H-^{13}C HSQC NMR spectroscopy (Figure 4), ^{13}C NMR spectra (Figure 3) was devoid of any peak corresponding to the carbonyl carbon of a ketone moiety. The absence of ketone signals in ^{13}C NMR could be explained in following way. The ketones (represented as **2** and **4** in Scheme 1) are reactive in presence of PAA and thus, possibly undergo Baeyer-Villiger oxidation (see following discussion for more details) as soon as they were produced. Consequently, they were not detected in the reaction medium or their concentration is negligible and fell below the detection limit of ^{13}C NMR spectroscopy. The reaction mechanism pertaining to C_α-C_β cleavage could be explained by Baeyer-Villiger oxidation of two possible ketones, such as **2** and **4,** by PAA, which produce phenolic acids as the products. It is important to note that Baeyer-Villiger oxidation of a ketone usually produces an ester as the product, but as the reaction was carried out in acid medium, the in situ generated ester underwent acid hydrolysis

and correspondingly, phenolic acid (**5**) was obtained as the final Figure 5) particularly with the lower amount of PAA, we concluded that the Baeyer-Villiger oxidation route is the predominant pathway for the PAA-mediated oxidative of depolymerisation of lignin. However, the comparable amount of (substituted) phenols obtained with 1 g PAA/g lignin product suggested that the side-chain replacement pathway becomes noteworthy to the overall oxidation when a large amount of PAA was used as oxidant. To demonstrate C_α-C_β bond cleavage through Baeyer-Villiger oxidation, we also performed oxidation of lignin model compounds whose structures, reactivity, and inter-unit linkages resemble the parent lignin polymer. The proposed complete reaction network corresponding to the Baeyer-Villiger oxidation of 4-methoxy acetophenone (**S1)** is summarised in Scheme S2. When **S1** was treated with PAA in the presence of acetic acid at 60°C for 2 h, 4-methoxyphenol (**S2**) and 4-methoxybenzoic acid (**S3**) were obtained as the amounts of 4-hydroxyphenol (**S4**) is attributed to the ether cleavage (-OCH_3) prior to the Baeyer-Villiger oxidation followed by hydrolysis. Though we propose that the carbonyl structure in compounds **2** and **4** was obtained through either oxidation of the benzylic alcohol or pinacol-pinacolone rearrangement, prior literature[65, 66] mentioned that the carbonyl in C_α is already present in some of the lignin structures and could directly undergo Baeyer-Villiger oxidation.

Based on the reaction mechanism discussed above, we conclude that side-chain replacement pathway requires one molecule of PAA to cleave one C-C linkage (C_α-C_{phenyl} in this case). On the other hand, side-chain oxidation pathway involved in the higher consumption of PAA likely consumed one molecule of PAA for C_α-C_β oxidative cleavage and another molecule can be consumed to oxidise the hydroxyl group on the propanyl side chain, as applicable. Hence, approximately 1-2 molecules of PAA are needed per lignin linkages to completely depolymerise lignin to monomeric phenolic products with quantitative yield. Using an excess amount of PAA (e.g. 1 g PAA/g lignin) resulted in 28 wt% MPC yield, slightly lower than the

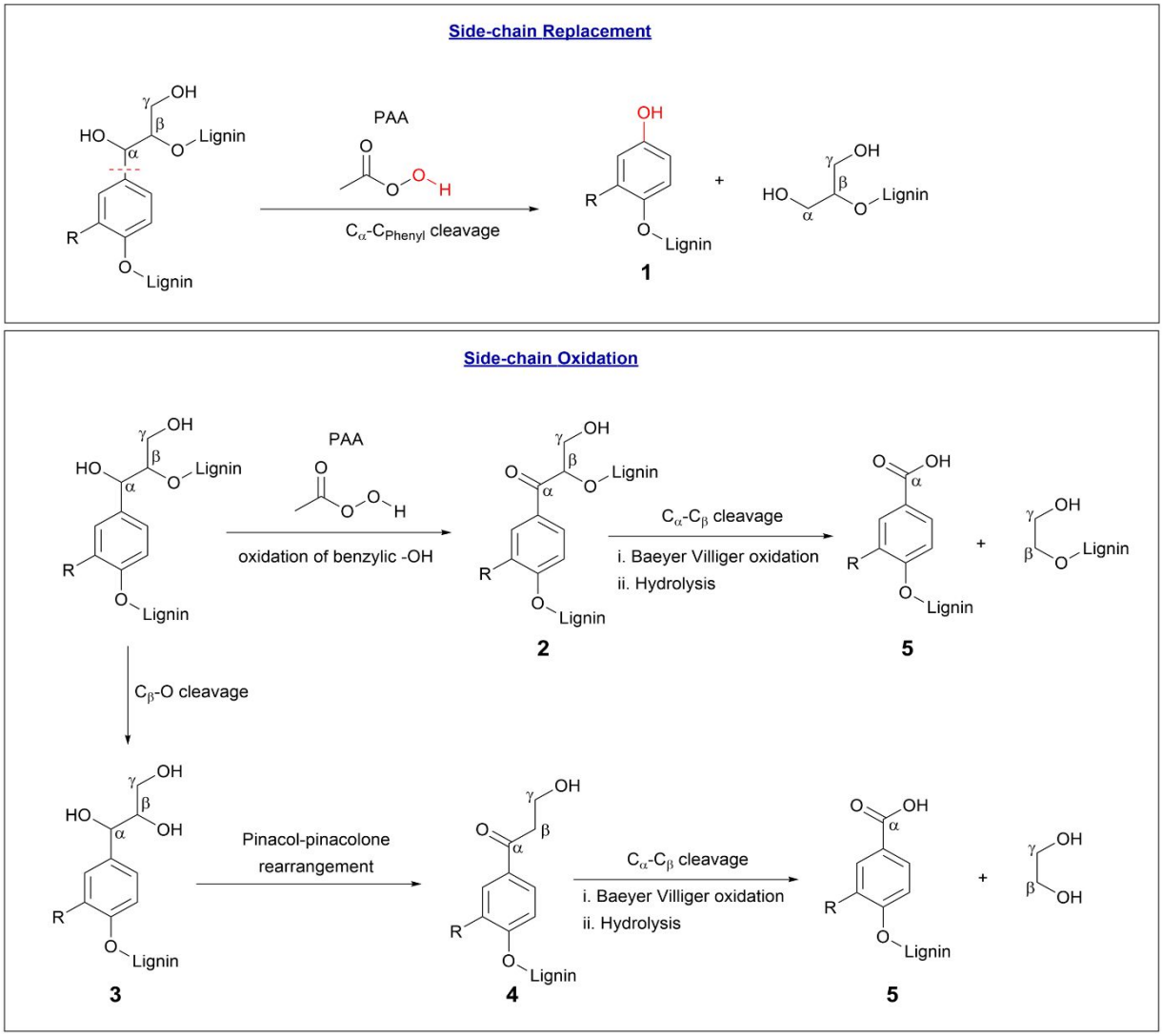

Scheme 1 The reaction network pertaining to the depolymerisation of DACSL in presence of PAA.

products. The formation of these products could be explained by the Baeyer-Villiger oxidation of **S1,** followed by the acid hydrolysis of the corresponding ester. The presence of small optimum 0.8 g PAA/g lignin, suggesting that the additional PAA was used in parasitic reactions not leading to MPC formation. (Note: Assuming each lignin monomeric unit has a molecular weight of 200

g/mol and has one linkage shared between another unit, 1 g PAA/g lignin is equivalent to 2.6 mole PAA per mole of lignin monomeric units.) The increasing amount of acidic side chain fragments with increased PAA dosage, as shown in Figure 5 (blue), suggests that PAA was being consumed for the oxidation of side-chain fragments (C2-C4) to the corresponding carboxylic acids (e.g., carboxylic acids, hydroxylated carboxylic acids, diacids). Further oxidation of the C-C bond of these carboxylic acids also generated C1-C2 acids and likely further contributed to the increased PAA consumption.

Effect of catalysts on PAA-mediated depolymerisation of lignin

Effect of different metal oxide catalysts was also investigated during the oxidative depolymerisation of lignin. We recently reported the promotional effect of niobium pentoxide (Nb_2O_5) during PAA-mediated depolymerisation of lignin to produce MPCs with total yield of ~47%.[35] Herein, we expanded our study to various other metal oxides and mixed metal oxides such as CuO, MnO_2, ZrO_2, SnO, 1% Mn on Nb_2O_5, 1% Mn on ZrO_2, 1% Re on Nb_2O_5, $CaCeO_2$, and hydrotalcite. CuO and MnO_2 were chosen based on their known high activity to activate peroxygen and thus could catalyse oxidation reactions. ZrO_2 and SnO were considered because of their different acid/base properties. The heterogeneous acid/base metal oxides were also utilised as support to anchor various active metal ions (e.g., Mn, Re). As Nb_2O_5 was identified as one of the active catalysts for oxidative depolymerisation of lignin, various mixed metal oxides based on Nb_2O_5 were also synthesised by wet impregnation and tested to identify potential synergistic effects. Mixtures of mixed metal oxides studied in the present work includes NbZr2575 (Nb_2O_5/ZrO_2; 25/75 wt%), NbZr5050 (Nb_2O_5/ZrO_2; 50/50 wt%), NbHT2575 (Nb_2O_5/Hydrotalcite; 25/75 wt%), NbHT5050 (Nb_2O_5/Hydrotalcite; 50/50 wt%), NbSn2575 (Nb_2O_5/SnO; 25/75 wt%), and NbSn5050 (Nb_2O_5/SnO; 50/50 wt%). Mixed metal oxide catalysts were obtained by preparing a physical mixture of corresponding metal oxide followed by calcination at 500°C for 4 h.

Total yield of phenolic compounds obtained from the PAA-mediated oxidative depolymerisation of lignin in the presence of different catalysts is shown in Figure 6. While Figure 6a compares the activity of different metal oxide catalysts, Figure 6b summarises the results obtained from Nb_2O_5 and Nb_2O_5-based mixed metal oxide catalysts. Yield of the depolymerisation reaction in the absence of catalysts was utilised as baseline. Comparing the results obtained in the absence of any catalysts (28 wt% yield), CuO and MnO_2 exhibited lower MPC yields (12 wt% and 27 wt%, respectively). More gas bubbles were generated upon addition of PAA to the reaction mixture. This observation could be attributed to the non-reactive oxygen evolution from PAA degradation in the presence of CuO and MnO_2, resulting in low MPC yields. Degradation of PAA was also invoked to explain the low activity of catalysts containing active metal ions supported on metal oxide compared to their parent metal oxides. On the other hand, ZrO_2 and SnO showed significant increase in MPC yields up to 37 wt%. However, Ca-CeO_2 and hydrotalcite exhibited only a small yield enhancement compared to pure PAA treatment, with yield of phenolic compounds at 28 wt% and 30 wt%, respectively. Among the tested catalysts, Nb_2O_5 remained as the most active in lignin depolymerisation to MPCs. Catalytic activities corresponding to Nb_2O_5-based mixed metal oxide catalysts that were prepared by blending ZrO_2, SnO, and hydrotalcite at different weight ratios were found to be similar as the bare Nb_2O_5 at the current reaction conditions. The total yield of the phenolic compounds was ranging from 31 to 46 wt%.

Although the total yield of the phenolic compounds was found similar across these catalysts, the trend in product selectivity was varied with the composition of the catalyst. Although no apparent activity trend was noted among the different catalysts, higher yield of phenolic compounds obtained in the presence of catalyst further evidenced its beneficial role during the oxidative depolymerisation of lignin.

The difference in both activity and product selectivity obtained with various metal oxide and mixed metal oxide

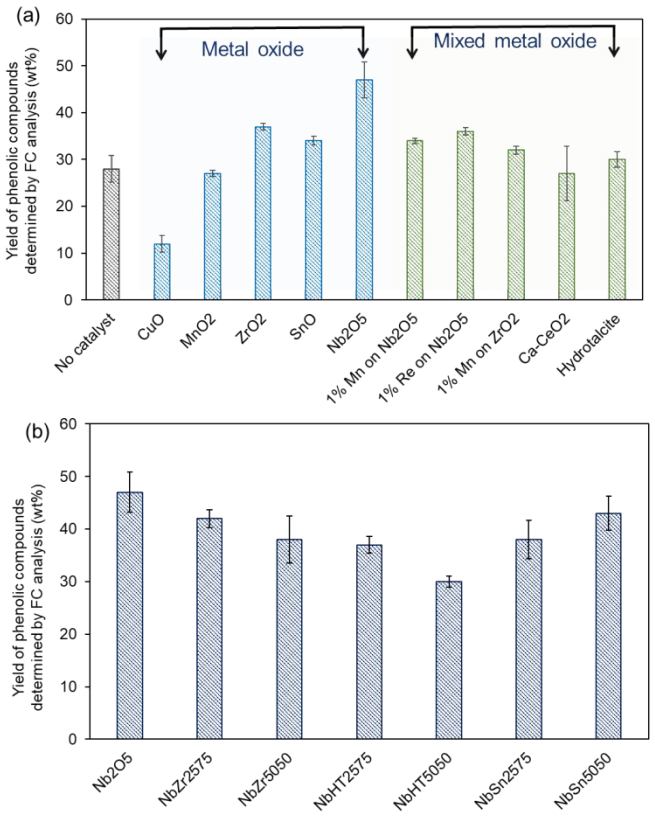

Figure 6. Yield of the phenolic compounds obtained during PAA-mediated oxidative depolymerisation reaction in presence of different catalysts. (a) Metal oxide and mixed metal oxide catalyst; (b) Nb_2O_5 and Nb_2O_5 based mixed metal oxide catalysts. Reaction condition - 1 g PAA/g lignin, 60°C, 5 h.

reported herein was attributed to their specific interaction with PAA and their ability to stabilise various intermediates generated during the lignin depolymerisation. The fundamental understanding of these aspects is beyond the scope of this work and will be explored elsewhere.

Preliminary techno-economic analysis

Developing market co-products from lignin is key to mitigating the fuel production cost from lignocellulosic biomass. PAA depolymerisation of lignin waste stream to selective MPCs presents a promising opportunity. We recognised that a considerable amount of PAA reagent (such as 1 g PAA/g lignin) at the scale utilised in this study may present an economic challenge. A preliminary techno-economic analysis was carried out to understand the key economic barriers of this process, with the aim of identifying key drivers that largely impact the economic viability of proposed process to produce MPC products. The analysis was based on integrating the lignin-to-MPC conversion process within an existing lignocellulose biomass-to-hydrocarbon fuel pathway developed by the National Renewable Energy Laboratory to determine the benefit of MPC co-products on final fuel production cost.[67] The analysis methodology, financial assumptions, capital and operating costs are similar to published technical reports.[67] Ten variable parameters, such as, PAA oxidant loading (0.2-2 g per g of lignin), MPC value (0.5-1.25 $/lb), MPC yield (30-60 wt%), solvent loading (acetic acid, 1-20 ml/g of lignin), solvent loss in recycle (0.1% to 3%), capex (-50% to +50%), MPC loss during liquid-liquid extractions (0 to 5%), extraction solvent loading (25% to 200%), catalyst cost (5 to 90 $/lb), and catalyst life (0.2 to 2 years), were considered in the sensitivity study and process economic analysis model. The variability of PAA loading, MPC yield, solvent loading was adapted from our experimental results presented herein. The range of the MPC value was chosen based on the cost of the products identified in our reaction condition. Similarly, catalyst cost variation considered in the analysis includes the cost of different catalysts shown in Figure 6. Based on this preliminary analysis, the oxidant consumption, selling price for the MPC product, MPC yield, and amount of solvent utilised during lignin deconstruction are the major cost drivers as illustrated in a tornado chart (Figure S9). The oxidant usage is observed to be the biggest cost driver (approximately -44% to +55%) because PAA was consumed during the reaction and its price is high. Based on previous work[35], oxidation using 1.0 g PAA/g lignin was considered as the base case scenario. Reducing PAA to 0.2 g per gram of lignin will result in a significant cost reduction (by 44%). Change in the MPC value between $0.5/lb to $1.25/lb resulted in -6% to +13% change, while MPC yield between 30% and 60% translated to a calculated fuel cost change of +6% and -10%. On the other hand, catalyst cost was not a key driver, generating negligible change in the model fuel cost when the price was varied between $5/lb to $90/lb. Thus, based on the preliminary TEA, the largest impact to the reduction of the over-all cost of the technology can be gained through developing strategies to decrease PAA usage while increasing MPC yield. On the other hand, the use of Nb_2O_5 as catalyst can still result in some cost reduction if the yield of MPC during the PAA mediated oxidative depolymerization of lignin is sufficiently improved.

Conclusions

The present study contributed to improved understanding of the underlying chemistry pertaining to the PAA-mediated oxidative depolymerisation of lignin macromolecule. Addition of PAA resulted in physical changes in lignin structure, exhibited by the swelling (expansion in volume) phenomenon followed by its complete solubilisation in different solvents. During this process, PAA oxidatively modifies the hydroxyl groups present in the propanyl side chain, which not only reduces the possibility for the formation of inter- and intra- molecular hydrogen bond, but also convert the hydroxyl groups into a bulkier functional group (e.g., carboxylic acids) that hinders the π-π interaction and disrupts the integrated packing structure. The structural changes of the lignin were further evidenced by powder XRD. ^{1}H-^{13}C HSQC NMR spectroscopy also shows that ether linkages between aromatic units are more susceptible to oxidation and likely to cleave at the initial stages of the depolymerisation. However, cleavage of the C_α-C_β bond was identified as the key parameter for the efficient depolymerisation of lignin. Based on the NMR characterisation along with product distribution, Baeyer-Villiger oxidation was determined to be the predominant reaction pathways for the PAA-mediated oxidative depolymerisation of lignin. Various metal oxides and mixed metal oxides were employed to improve the efficiency of depolymerisation and the yield of the phenolic compounds. Based on the preliminary techno-economic analysis, it is evident that reduction of the oxidant (PAA) usage is important to make the overall PAA depolymerisation process cost effective. As catalyst cost does not impact the overall economics significantly, judicious choice of the catalyst provides a viable option to develop an efficient process.

Author contribution

The manuscript was written through contributions of all authors. All authors have given approval to the final version of the manuscript.

Corresponding Authors:

*X. Zhang. E-mail: x.zhang@wsu.edu; xiao.zhang1@pnnl.gov; M.V. Olarte. E-mail: mariefel.olarte@pnnl.gov.

Conflicts of interest

There are no conflicts to declare.

Acknowledgements

The authors thank Dr. Karthi Ramasamy and Dr. Asanga Padmaperuma for internal peer-review and scientific discussion; Ms. Jan Haigh for technical editing and Mr. Mike Perkins for illustration. The authors gratefully acknowledge the financial supports from the Bioenergy Technologies Office of the U.S. Department of Energy (Contract no: DE-AC06-76RLO-

1830) as well as National Science Foundation (Award no: 1454575) and U.S. Federal Aviation Administration (FAA) Office of Environment and Energy under 13-C-AJFE-WaSU ASCENT project COE-2014-01. A portion of the research was performed using PNNL's Environmental Molecular Science Laboratory (grid.436923.9), a DOE Office of Science User Facility sponsored by the Biological and Environmental Research program. We also thank Kristin C. Lewis and Nathan Brown from FAA for providing suggestion to this work.

References

1. A. J. Ragauskas, G. T. Beckham, M. J. Biddy, R. Chandra, F. Chen, M. F. Davis, B. H. Davison, R. A. Dixon, P. Gilna and M. Keller, *Science*, 2014, **344**, 1246843.
2. W. Schutyser, T. Renders, S. Van den Bosch, S.-F. Koelewijn, G. T. Beckham and B. F. Sels, *Chemical Society Reviews*, 2018, **47**, 852-908.
3. R. Ma, M. Guo and X. Zhang, in *Lignin Valorization*, 2018, pp. 128-158.
4. R. Ma, M. Guo and X. Zhang, *Catalysis Today*, 2018, **302**, 50-60.
5. R. Ma, Y. Xu and X. Zhang, *ChemSusChem*, 2015, **8**, 24-51.
6. S. Guadix-Montero and M. Sankar, *Topics in Catalysis*, 2018, **61**, 183-198.
7. R. Rinaldi, R. Jastrzebski, M. T. Clough, J. Ralph, M. Kennema, P. C. Bruijnincx and B. M. Weckhuysen, *Angewandte Chemie International Edition*, 2016, **55**, 8164-8215.
8. C. Xu, R. A. D. Arancon, J. Labidi and R. Luque, *Chemical Society Reviews*, 2014, **43**, 7485-7500.
9. J. Zakzeski, P. C. Bruijnincx, A. L. Jongerius and B. M. Weckhuysen, *Chemical reviews*, 2010, **110**, 3552-3599.
10. S. Ghysels, B. Dubuisson, M. Pala, L. Rohrbach, J. Van den Bulcke, H. J. Heeres and F. Ronsse, *Green Chemistry*, 2020, **22**, 6471-6488.
11. R. B. Santos, P. Hart, H. Jameel and H.-m. Chang, *BioResources*, 2013, **8**, 1456-1477.
12. J. Gierer, *Wood Science and Technology*, 1986, **20**, 1-33.
13. J. Gierer, *Wood Science and Technology*, 1980, **14**, 241-266.
14. X. Zhang, M. Tu and M. G. Paice, *BioEnergy Research*, 2011, **4**, 246-257.
15. D. Fengel and G. Wegener, *Wood: chemistry, ultrastructure, reactions*, Walter de Gruyter, 1983.
16. W. Schutyser, J. S. Kruger, A. M. Robinson, R. Katahira, D. G. Brandner, N. S. Cleveland, A. Mittal, D. J. Peterson, R. Meilan and Y. Román-Leshkov, *Green Chemistry*, 2018, **20**, 3828-3844.
17. T. Vangeel, W. Schutyser, T. Renders and B. F. Sels, *Topics in Current Chemistry*, 2018, **376**, 30.
18. C. Liu, S. Wu, H. Zhang and R. Xiao, *Fuel Processing Technology*, 2019, **191**, 181-201.
19. L. Shuai, M. T. Amiri, Y. M. Questell-Santiago, F. Héroguel, Y. Li, H. Kim, R. Meilan, C. Chapple, J. Ralph and J. S. Luterbacher, *Science*, 2016, **354**, 329-333.
20. A. Rahimi, A. Ulbrich, J. J. Coon and S. S. Stahl, *Nature*, 2014, **515**, 249.
21. E. M. Anderson, R. Katahira, M. Reed, M. G. Resch, E. M. Karp, G. T. Beckham and Y. Román-Leshkov, *ACS Sustainable Chemistry & Engineering*, 2016, **4**, 6940-6950.
22. J. Dai, A. F. Patti, L. Longé, G. Garnier and K. Saito, *ChemCatChem*, 2017, **9**, 2684-2690.
23. Y. Sun, H. Ma, Y. Luo, S. Zhang, J. Gao and J. Xu, *Chemistry–A European Journal*, 2018, **24**, 4653-4661.
24. S. Dabral, J. G. Hernández, P. C. Kamer and C. Bolm, *ChemSusChem*, 2017, **10**, 2707-2713.
25. R. S. Weber and K. K. Ramasamy, *ACS Omega*, 2020, **5**, 27735-27740.
26. D. Di Marino, V. Aniko, A. Stocco, S. Kriescher and M. Wessling, *Green Chemistry*, 2017, **19**, 4778-4784.
27. E. Reichert, R. Wintringer, D. A. Volmer and R. Hempelmann, *Physical Chemistry Chemical Physics*, 2012, **14**, 5214-5221.
28. S. Stiefel, A. Schmitz, J. Peters, D. Di Marino and M. Wessling, *Green Chemistry*, 2016, **18**, 4999-5007.
29. T. Akiyama, T. Sugimoto, Y. Matsumoto and G. Meshitsuka, *Journal of Wood Science*, 2002, **48**, 210-215.
30. H. Kaneko, S. Hosoya, K. Iiyama and J. Nakano, *Journal of Wood Chemistry and Technology*, 1983, **3**, 399-411.
31. C. Zhang, P. J. B. Brown and Z. Hu, *Science of The Total Environment*, 2018, **621**, 948-959.
32. D. J. Cronin, K. Dunn, X. Zhang and W. O. Doherty, *ACS Sustainable Chemistry & Engineering*, 2017, **5**, 11695-11705.
33. D. J. Cronin, X. Zhang, J. Bartley and W. O. Doherty, *ACS Sustainable Chemistry & Engineering*, 2017, **5**, 6253-6260.
34. J. A. Jennings, S. Parkin, E. Munson, S. P. Delaney, J. L. Calahan, M. Isaacs, K. Hong and M. Crocker, *RSC Advances*, 2017, **7**, 25987-25997.
35. R. Ma, M. Guo, K. t. Lin, V. R. Hebert, J. Zhang, M. P. Wolcott, M. Quintero, K. K. Ramasamy, X. Chen and X. Zhang, *Chemistry-A European Journal*, 2016, **22**, 10884-10891.
36. R. Ma, M. Guo and X. Zhang, *ChemSusChem*, 2014, **7**, 412-415.
37. Y. Wang, Q. Wang, J. He and Y. Zhang, *Green Chemistry*, 2017, **19**, 3135-3141.
38. N. D. Patil, S. G. Yao, M. S. Meier, J. K. Mobley and M. Crocker, *Organic & biomolecular chemistry*, 2015, **13**, 3243-3254.
39. W. J. Lawrence, R. D. McKelvey and D. C. Johnson, 1978.
40. P. Sun, T. Zhang, B. Mejia-Tickner, R. Zhang, M. Cai and C.-H. Huang, *Environmental Science & Technology Letters*, 2018, **5**, 400-404.
41. C. A. Bettenhausen, *Chemical and Engineering News*, 2020, **98**.
42. T. Renders, S. Van den Bosch, S.-F. Koelewijn, W. Schutyser and B. Sels, *Energy & Environmental Science*, 2017, **10**, 1551-1557.

43. X. Chen, J. Shekiro, T. Pschorn, M. Sabourin, L. Tao, R. Elander, S. Park, E. Jennings, R. Nelson and O. Trass, *Biotechnology for Biofuels*, 2014, **7**, 98.
44. R. Ma, X. Zhang, Y. Wang and X. Zhang, *ChemSusChem*, 2018, **11**, 2146-2155.
45. A. Sluiter, B. Hames, R. Ruiz, C. Scarlata, J. Sluiter, D. Templeton and D. Crocker, *Laboratory analytical procedure*, 2008, **1617**, 1-16.
46. A. Sluiter, B. Hames, R. Ruiz, C. Scarlata, J. Sluiter, D. Templeton and D. Crocker, *Laboratory analytical procedure*, 2008, **1617**.
47. A. Medina-Remón, A. Barrionuevo-González, R. Zamora-Ros, C. Andres-Lacueva, R. Estruch, M.-Á. Martínez-González, J. Diez-Espino and R. M. Lamuela-Raventos, *Analytica Chimica Acta*, 2009, **634**, 54-60.
48. V. L. Singleton, R. Orthofer and R. M. Lamuela-Raventós, in *Methods in enzymology*, Elsevier, 1999, vol. 299, pp. 152-178.
49. S. D. Mansfield, H. Kim, F. Lu and J. Ralph, *Nature protocols*, 2012, **7**, 1579.
50. D. Meier, O. Faix, S. Lin and C. Dence, *Methods in Lignin chemistry*, 1992.
51. R. El Hage, N. Brosse, L. Chrusciel, C. Sanchez, P. Sannigrahi and A. Ragauskas, *Polymer Degradation and Stability*, 2009, **94**, 1632-1638.
52. W. Boerjan, J. Ralph and M. Baucher, *Annual review of plant biology*, 2003, **54**, 519-546.
53. Y.-R. Chen and S. Sarkanen, *Phytochemistry reviews*, 2003, **2**, 235-255.
54. Y.-Y. Wang, Y.-r. Chen and S. Sarkanen, *Green Chemistry*, 2015, **17**, 5069-5078.
55. Y.-R. Chen and S. Sarkanen, in *Characterization of Lignocellulosic Materials*, Blackwell Publishing Ltd, 2009.
56. Y. Li and S. Sarkanen, *Macromolecules*, 2005, **38**, 2296-2306.
57. J. Ralph and L. L. Landucci, *Lignin and lignans: advances in chemistry*, 2011.
58. A. Rahimi, A. Azarpira, H. Kim, J. Ralph and S. S. Stahl, *Journal of the American Chemical Society*, 2013, **135**, 6415-6418.
59. E. Adler, *Wood science and technology*, 1977, **11**, 169-218.
60. D. C. Johnson and J. C. Farrand, *The Journal of Organic Chemistry*, 1971, **36**, 3606-3612.
61. G. X. Pan, L. Spencer and G. J. Leary, *Journal of agricultural and food chemistry*, 1999, **47**, 3325-3331.
62. K. Kervinen, H. Korpi, M. Leskelä and T. Repo, *Journal of Molecular Catalysis A: Chemical*, 2003, **203**, 9-19.
63. S. Son and F. D. Toste, *Angewandte Chemie International Edition*, 2010, **49**, 3791-3794.
64. J. Zakzeski, A. Dębczak, P. C. A. Bruijnincx and B. M. Weckhuysen, *Applied Catalysis A: General*, 2011, **394**, 79-85.
65. C.-L. Chen, in *Methods in Lignin Chemistry*, eds. S. Y. Lin and C. W. Dence, Springer Berlin Heidelberg, Berlin, Heidelberg, 1992, DOI: 10.1007/978-3-642-74065-7_30, pp. 446-457.
66. R. Katahira, T. J. Elder and G. T. Beckham, in *Lignin Valorization: Emerging Approaches*, The Royal Society of Chemistry, 2018, DOI: 10.1039/9781788010351-00001, pp. 1-20.
67. R. Davis, L. Tao, E. C. D. Tan, M. J. Biddy, G. T. Beckham, C. Scarlata, J. Jacobsen, K. Cafferty, J. Ross, J. Lukas, D. Knorr and P. Schoen, *NREL/TP-5100-60223, National Renewable Energy Laboratory, October 2013.* https://www.nrel.gov/docs/fy14osti/60223.pdf.